In Vivo Breast Cancer Measurement with a Handheld Laser Breast Scanner

Keun Sik No, Qiang Xie, and Pai H. Chou
Department of Electrical Engineering & Computer Science
University of California, Irvine, CA 92697 USA
Email: {kno, qxie, phchou}@uci.edu

Richard Kwong, Albert Cerussi, and Bruce J. Tromberg
Beckman Laser Institute and Medical Clinic
University of California, Irvine, CA 92697 USA
Email: {rykwong, acerussi, bjtrombe}@uci.edu

***Abstract*— HBS is a handheld system for noninvasive breast cancer detection based on frequency domain photon migration. It performs broadband modulation on near-infrared laser intensity and derives the scattering and absorption coefficients from phase and amplitude measurements. Recovered optical properties of phantom and tissue by HBS clearly show the difference between normal and cancer tissue. Measurements show HBS can replace the current prototype while costing a small fraction.**

I. Introduction

Diffuse optical spectroscopy (DOS) has been used to detect breast cancer. Specifically, frequency domain photon migration (FDPM) DOS methods have been successful at non-invasive, content-based detection of breast tumors to complement image-based techniques[1]. FDPM works by beaming near-infrared (NIR) light that has been modulated from 10MHz to 1GHz into a tissue and measures the amplitude and phase differences of the backscattered light. Then, by fitting the amplitude and phase data to diffusion theory approximation, it can extract optical properties in terms of absorption coefficient μ_a and scattering coefficient, μ_s'[2]. Currently, prototypes for FDPM measurement called the Laser Breast Scanner (LBS) have been constructed at the Beckman Laser Institute (BLI) and been used in clinical trials[3]. However, the LBS is bulky and expensive, because it is constructed with a general-purpose network analyzer and laser drivers. The generality and loose coupling also unnecessarily increase the whole measurement time.

II. Device

We have designed the HBS system, a handheld instrument that aims to replace the LBS without sacrificing accuracy[4]. Fig. 1 shows the lastest schematic. It has four laser diodes whose power can be controlled by a microcontroller. To generate 10MHz to 1GHz signals, we used 2–2.99GHz and 3GHz phase-locked loop voltage controlled oscillators (PLL VCOs). By mixing the output of these two PLL VCOs and filtering, we can generate lower broadband frequencies. Another 1.955–2.945GHz PLL VCO is used to generate a heterodyne 45MHz signal. The heterodyne structure filters out unwanted and noise signals within the band using a crystal filter combined with lumped components that form a low pass filter (LPF). Using 1.955–2.945GHz PLL VCO first at the detection path eliminates the leaky signal by choosing the frequency bands of both the broadband and local oscillators to be far outside the generated band by upconverting the demodulated signal. With the IF signal from the APD, HBS generates a 2.955GHz LO signal, which is a high intermediate frequency. This LO signal goes through the filter and the amplifier and is mixed as RF with the 3GHz LO to generate the 45MHz detection signal. The 1GHz LPF can effectively prevent this RF signal from leaking out of the system. The maximum power we can use to modulate a laser is around 20dBm and is controllable by a programmable attenuator. The whole system is controlled by a 16-bit microcontroller over an Ethernet connection from a host computer. Measurement results with tissue-like phantoms have shown that HBS captures data similar to the gold-reference LBS with a maximum 7.5% difference, while cutting the measurement time down to 0.5s, or 1/10 of the current LBS [5]. Fig. 1 and Fig. 2 show the schematic and photo of the HBS structure.

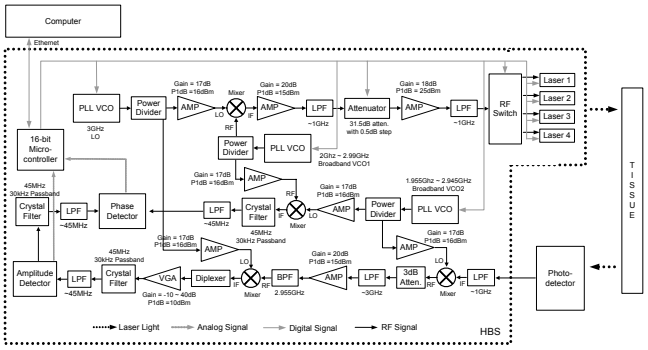

Fig. 1. Block diagram of the HBS.

A. Filter Design

The HBS uses ceramic filters from Mini-Circuits. We can use multiple chip filters in series due to the small chip filter dimension($3\times2\text{mm}^2$), unlike the microstrip line filter. A single unit may not satisfy the required specification, but multiple units composed in series may be able to achieve the required performance. Fig. 3 shows the measured S21 parameters of one, two, and three 1GHz LPFs with series connection. It shows that three 1GHz LPFs have better rejection ratio. Although passband loss is also increased, it is relatively small

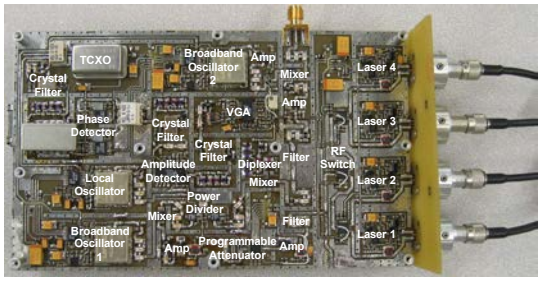

(a)

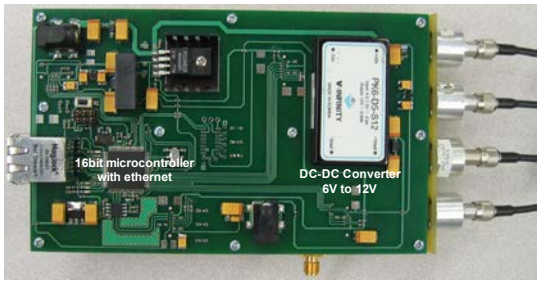

(b)

Fig. 2. (a) Front and (b) Back photo of the HBS.

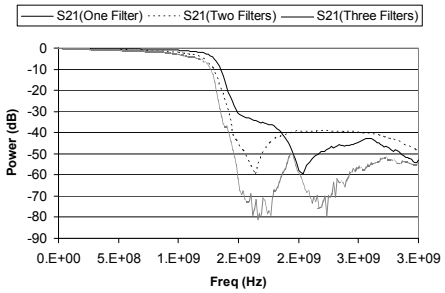

Fig. 3. Measured S21 of one, two, and three series 1GHz LPFs.

at about 1.5dB more and can be compensated.

The five filters used in the HBS are 1GHz, 3GHz, and 45MHz LPFs, a 2.955GHz BPF, and a 45MHz diplexer. Fig. 4 shows the passband and insertion losses of the 1GHz LPF, which is constructed with three 1GHz ceramic filters (the LFCN-1000 from Mini-Circuits). This filter is used to suppress the 2–3GHz frequencies with average 34.2dB. The 3GHz LPF is made with three 3GHz ceramic filters (LFCN-3000 from Mini-Circuits), and its passband and insertion losses are shown in Fig. 5. It suppresses the 4–6GHz frequencies, which are the 2nd harmonic frequencies of the signal generators with average 57dB. Fig. 6 shows the passband and insertion losses of the 2.955GHz BPF, which is made with two 2.7GHz HPFs (HFCN-2700 from Mini-Circuits) and two 3GHz LPFs (LFCN-3000). This is a bandpass filter to pass 2.955 GHz while rejecting other unwanted frequencies, specially 10MHz – 1GHz and 4–6GHz frequencies. The loss of 2.955GHz is 3.1dB and the rejection is 43.1dB and 32.1dB at lower and higher bands, respectively.

The 45MHz LPF and diplexer are designed with ADS. The

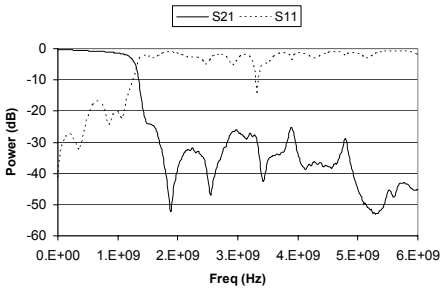

Fig. 4. Measured S21 and S11 of 1GHz LPF.

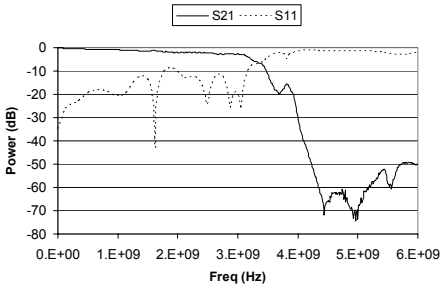

Fig. 5. Measured S21 and S11 of 3GHz LPF.

reasons are that there exist no products at the exact required frequency range, and they can be designed with lumped components in a small space with good agreement between simulation and real results. The 45MHz LPF is designed as a 9th Chebyshev with 0.1-dB ripple in the passband and 40dB rejection loss at 75MHz. The designed lumped component values are shown in Fig. 7(a). For better agreement between simulated and real results, high-Q inductors are used. Fig. 7(b) shows the simulated and measured value of S21 and S11 parameters. The measured passband and rejection losses are 1.7dB and 56.7dB, respectively. The diplexer is used after the second mixer on the detection path. This is for suppression of unwanted signal higher than 45MHz and for matching at the higher frequency band, so that it will be dissipated in the diplexer rather than reflecting back to the detection path. The lower band part (port2) and higher band part (port3) are designed as a 9th Chebyshev with 0.1-dB ripple in the

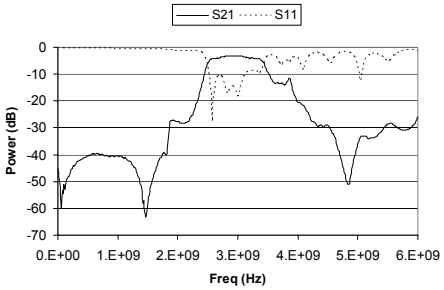

Fig. 6. Measured S21 and S11 of 2.955GHz BPF.

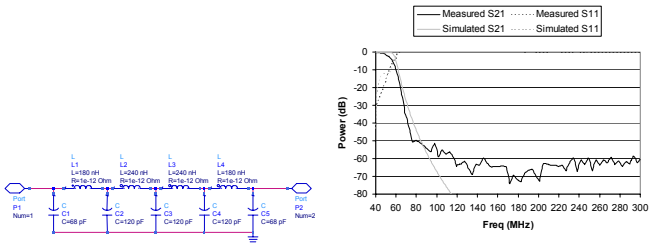

(a) (b)

Fig. 7. (a) Design value of 45MHz LPF (b) Simulated and Measured S parameters of 45MHz LPF.

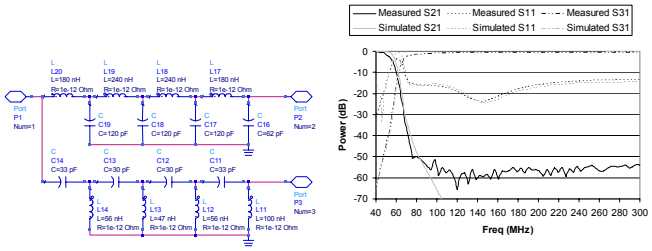

(a) (b)

Fig. 8. (a) Design value of 45MHz diplexer (b) Simulated and Measured S parameters of 45MHz diplexer.

passband. The designed values are shown in Fig. 8(a). Fig. 8(b) shows the simulated and measured values of S21 and S11 parameters of the diplexer.

III. Measurements

The measurement setup is shown in Fig. 9 for HBS. The four laser diodes (681, 783, 823, and 850nm) are run sequentially at 20mW optical power for the Full-heterodyne HBS. An optical fiber bundle with four 400μm diameter fibers is coupled to the four laser sources. The Hamamatsu C5658 avalanche photodiode detector and the optical fiber bundle are attached with variable distances on the tissue-simulating phantom or human tissue. Each laser is modulated from 50MHz to 300MHz in 1MHz steps at the maximum available power without saturating the modulation at the 50MHz frequency.

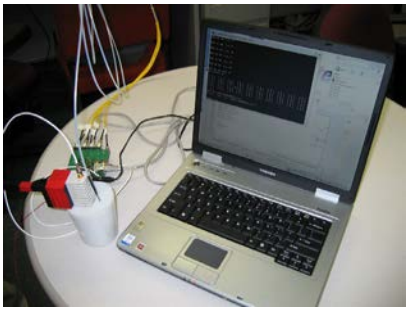

Fig. 9. Measurement setup.

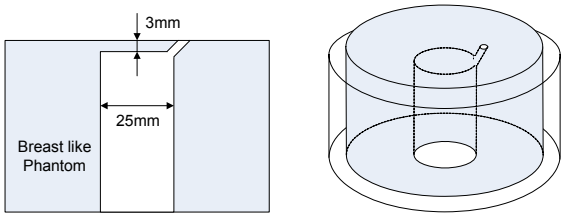

(a) (b)

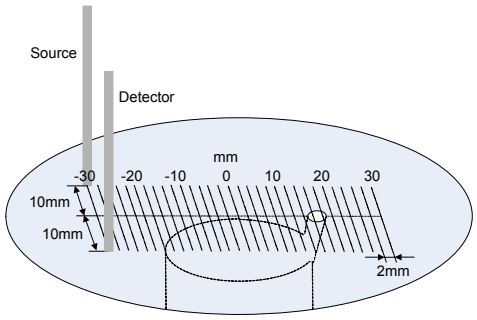

(c)

Fig. 10. (a) Schematic, (b) Measurement setup, and (c) Measurement spots of Tumor-in-Breast phantom.

A. Phantom measurement

Before measuring a patient, we first measured a simulated tumor in a breast phantom whose schematic is shown in Fig. 10(a). It looks like a regular phantom, but it has a hole in the center with a 25mm diameter. This place can be filled by a tumor-like liquid phantom. Fig. 10(b) shows the measurement setup of the tumor-in-breast phantom. We put this phantom into the beaker and filled it with the tumor-like liquid until we saw the liquid coming out of the small air vent at the top. We took measurements on this phantom along a straight line in steps of 2mm from -30mm to $+30$mm relative to the center of the phantom as the origin. It is shown in Fig. 10(c). The source/detector separation is 20mm with optical fiber coupling to the APD. The hole in the solid phantom was filled with a tumor-like liquid phantom whose optical properties are 0.022 and 1.2 for for μ_a and μ_s', respectively, and PH010 is used for reference phantom.

From the measurement results, we can see the difference within the positions. The extracted absorption coefficients at the center are almost double those at the edge. Fig. 11 shows the extracted optical properties along the X axis. All extracted optical properties from four lasers show clear differences between the center and the edge regions. At the region of the center, absorption coefficient is higher due to the high absorption coefficient of the tumor-like liquid phantom, and the scattering coefficient is lower for the same reason. For the scattering coefficient, we can observe a small inflection around the air vent. The scattering coefficient is sensitive to the structural difference. This phenomenon can be applied to detect homogeneity at a solid structure. The *full width at half maximum* (FWHM) can be calculated and is around 24.8mm, which is almost identical to the real diameter.

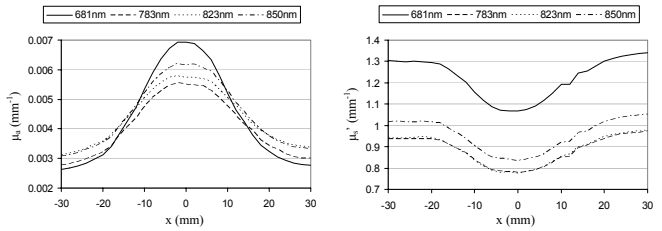

(a) (b)

Fig. 11. (a) Absorption and (b) Scattering coefficients of Tumor-in-Breast phantom with X axis.

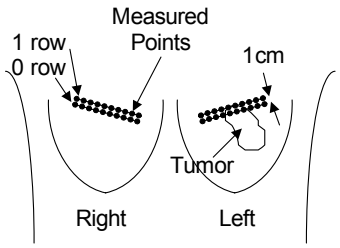

Fig. 12. Measurement points on the patient's breasts.

B. In vivo breast measurement

We measured one of the patients with breast cancer at the BLI Medical Clinic and this experiment were performed under the guidelines of UC Irvine TRB-approved protocol 95-563. The patient is a 59-year-old postmenopausal female with invasive ductal carcinoma in her left breast. The tumor lesion is at the center of the upper hemisphere of the left breast. The tumor size is 6.36 $\times$ 4.09cm, and the depth is approximately 0.5cm. She had started chemotherapy 6 days earlier and was still receiving chemotherapy at the time of our measurement. Fig. 12 shows the measurement points and the position of the tumor. For each breast, we used the HBS to measure 20 points that were organized as two rows of 10 points with a 28mm source/detector separation. Fig. 13 shows the extracted absorption coefficients of the breasts at the measurement points. The absorption coefficients around the center of the left breast are higher than those in the right breast due to the tumor. The tumor legion has enhanced blood supply, and NIR is highly absorbed by blood. So, the tumor legion has higher absorption coefficients than normal tissue [6], [7].

IV. Conclusions

This paper presents a miniature instrument for non-invasive, optical, content-based cancer detector based on FDPM. Our HBS system performs active sensing by emitting a broadband modulated laser light and measures the backscattered light in terms of amplitude and modulation phase shift. Measured amplitude and phase differences by HBS were accurate enough to recover optical properties of phantom or tissue. This form factor and performance are expected to enable this non-invasive, effective breast cancer detection method to gain much wider use.

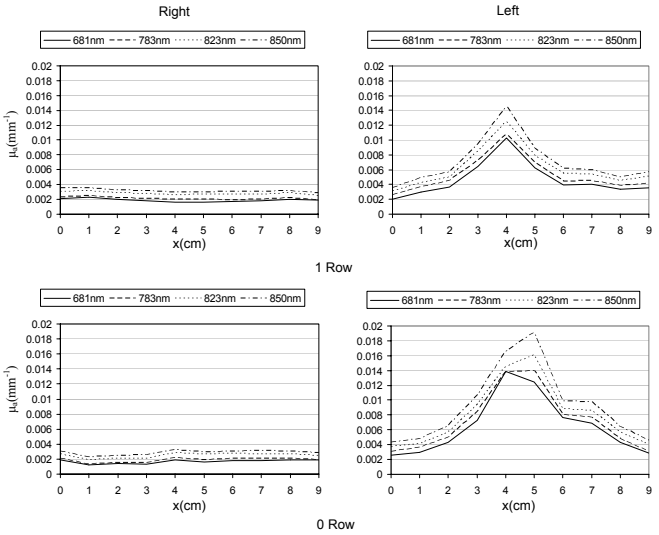

Fig. 13. Extracted absorption coefficients of breasts at measurement points.

V. Acknowledgments

This work was supported in part by the National Science Foundation (NSF) under NSF CAREER Grant CNS-0448668, by a Henry T. Nicholas Fellowship (for K.S. No), by the National Institute of Health (NIH) under the Network for Translational Research in Optical Imaging (NTROI) Seed Grant, and by the National Institutes of Health under grants SBIR 34337, U54-CA105480 (NTROI), P41-RR01192 (Laser Microbeam and Medical Program: LAMMP).

References

[1] B. J. Tromberg, N. Shah, R. Lanning, A. Cerussi, J. Espinoza, T. Pham, L. Svaasand, and J. Butler, "Non-invasive *In Vivo* characterization of breast tumors using photon migration spectroscopy," *Neoplasia*, vol. 2, no. 1–2, pp. 26–40, Jan.–Apr. 2000.

[2] R. C. Haskell, L. O. Svaasand, T.-T. Tsay, T.-C. Feng, M. S. McAdams, and B. J. Tromberg, "Boundary conditions for the diffusion equation in radiative transfer," *Optical Society of America*, vol. 11, no. 10, pp. 2727–2741, October 1994.

[3] A. Cerussi, N. Shah, D. Hsiang, A. Durkin, and B. J. Tromberg, "*In vivo* absorption, scattering, and physiologic properties of 58 malignant breast tumors determined by broadband diffuse optical spectroscopy," *Journal of Biomedical Optics*, vol. 11, no. 4, pp. 0 440 051–04 400 516, August 2006.

[4] K.-S. No and P. H. Chou, "Mini-FDPM and Heterodyne Mini-FDPM: Handheld non-invasive breast cancer detectors based on frequency-domain photon migration," *IEEE Transactions on Circuits and Systems*, vol. 52, pp. 2672–2685, 2005.

[5] K.-S. No, Q. Xie, R. Kwong, A. Cerussi, B. J. Tromberg, and P. H. Chou, "HBS: a handheld breast cancer detector based on frequency domain photon migration with full heterodyne," in *Proc. IEEE Biomedical Circuits and Systems*, vol. 2, 2006, pp. 3.2–10–3.2–14.

[6] S. Fantini, S. A. Walker, M. A. Franceschini, M. Kaschke, P. M. Schlag, and K. T. Moesta, "Assessment of the size, position, and optical properties of breast tumors in vivo by noninvasive optical methods," *Applied Optics*, vol. 37, no. 10, pp. 1982–1992, April 1998.

[7] M. A. Franceschini, K. T. Moesta, S. Fantini, G. Gaida, E. Gratton, H. Jess, W. W. Mantulin, M. Seeber, P. M. Schlag, and M. Kaschke, "Frequency-domain techniques enhance optical mammography: Initial clinical results," *Proceedings of the National Academy of Sciences*, vol. 94, pp. 6468–6473, June 1997.